

LIST OF PUBLICATIONS

- 1) Samor Boonphan and Pisith Singjai, Effect of step-heating on microstructure and mechanical properties of linear low density polyethylene/multi-walled carbon nanotube composites prepared via melt mixing process, *AMR.*, 2014, Volume 979, Pages 107–110.
- 2) Samor Boonphan and Pisith Singjai, Solar heat absorbing coating from multi-walled carbon nanotube composites with linear low-density polyethylene-coated copper sheet, *J Rein. Plas. Compo.*, 2017, Volume 36, Pages 714–721.



ลิขสิทธิ์มหาวิทยาลัยเชียงใหม่
Copyright© by Chiang Mai University
All rights reserved

Effect of step-heating on microstructure and mechanical properties of linear low density polyethylene/multi-walled carbon nanotube composites prepared via melt mixing process

Samor Boonphan^{1,a} and Pisith Singjai^{1,b*}

¹Department of Physics and Materials Science, Faculty of Science,
Chiang Mai University, Chiang Mai, 50200, Thailand

^asamor_b@hotmail.com, ^bpisith.s@cmu.ac.th

Keywords: Composites; Nanotubes; Mechanical Properties; Microscopy

Abstract. Step-heating (single- and four-step heating) was used in the melt-mixing preparation of linear low density polyethylene (LLDPE)/multi-walled carbon nanotube (MWNT) composites. The MWNT in the composites were used at volume fractions of 0, 1, 3, 5, and 10 vol% (four-step heating), and 0, 1, 3, and 5 vol% (single-step heating). The effects of the heating steps on the microstructure of the LLDPE/MWNT composites were studied. An ultimate tensile testing machine and an impact testing machine were used to characterize the mechanical properties of the composites. The sample prepared using four-step heating had a lower porosity than the sample prepared using single-step heating. The sample with 3 vol% MWNT that was prepared using four-step heating had tensile strength, elastic modulus, and impact strength values that were higher than those of the other samples.

Introduction

CNTs have been shown to have excellent mechanical properties, with a tensile strength of approximately 10 – 60 GPa, and a Young's modulus of approximately 0.3 – 1 TPa [1]. Polymer/CNT composites are very interesting. Polymers are light, cheap, and tough, but have poor mechanical properties; many scientists therefore use CNTs to fill polymers and improve their mechanical properties, to provide a replacement material for wood or metal. Kundu et al. studied the effects of various methods for the preparation of LLDPE films [2]. The film preparation procedures were varied, including variations in the cooling methods; quenching, forced cooling (by fan), and natural cooling were used. Naturally cooled samples showed the highest Young's modulus.

In this study, the mechanical properties of LLDPE/MWNT composites were studied after the application of single-step and four-step heating in the melt mixing process in furnace. The volume fraction of MWNT in the composite materials was varied, with 1, 3, 5, and 10 vol% used for four-step heating, and 1, 3, and 5 vol% used in single-step heating. Because of melt mixing process in furnace is suitable for the easy shape product and can produce many products in once. Therefore, this method was used in this study.

Experimental

MWNT were synthesized at the Nanomaterials Science Research Unit, Faculty of Science, Chiang Mai University, using the CVD method [3]. The length of the MWNT was more than 10 μm , and the average diameter was approximately 40 nm. Melt mixing process [4] was used in this study; the MWNT were mixed with LLDPE powder at 1, 3, 5 and 10 vol%, and were ball milled for 5h, to mix the samples. The samples were then melted in a furnace (Daihan Lab Tech Co.Ltd.) using

single-step heating—where the temperature was increased from room temperature to 170 °C in air, over a period of 5h, with a heating rate of 10 °C/min—and four-step heating (95 °C, 1h→125 °C, 2h→145 °C, 2h→170 °C, 10 min). FE-SEM (JSM 6335 F) was used to study the distribution of MWNT in the LLDPE matrix. An ultimate tensile testing machine (Hounsfield, Model H10KS) was used to study the mechanical properties of the LLDPE/MWNT composites, follow the ASTM D638-10 and strain rate of 50 mm/min. An impact tester (charpy) machine (Toolquip, Leicester LE67 5FT: England) was used to studied the impact strength of the LLDPE/MWNT composites prepared using single- and four-step heating, following ASTM D6110-10.

Results and Discussion

A mechanism that describes this process using a densification coefficient was suggested by the Scherer and Scherer and Garino models [5]. The coefficient depends on the bulk density and specific surface energy of the compact polymer. In other words, the reduction of the specific surface energy that occurs with increases in the temperature causes the air inside the open pores to be removed from the compact polymer, and the pores are thus closed. This model describes the behavior well until the closed pores form, which occurs at $\rho/\rho_s = 0.942$, where ρ is the polymer density and ρ_s is the full density of the polymer. After the pores are closed, the viscosity of the polymer melt decreases as the temperature increases. Because the viscosity of the polymer melts decreases, the polymer chains in the melt become shorter [6], which means that the diffusion of air through the polymer melts becomes easier. In addition, the pressure of the hot air inside the bubbles increases, causing the diffusion rate of the air to increase [7], as suggested by the diffusion model.

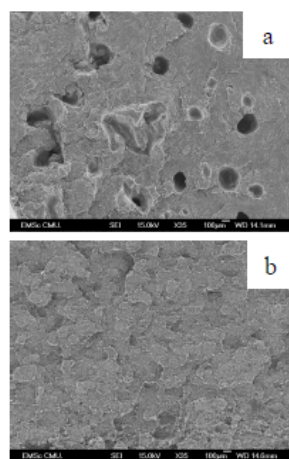


Fig. 1 (a) Single-step heating and (b) four-step heating of the sample at 5 vol% MWNT

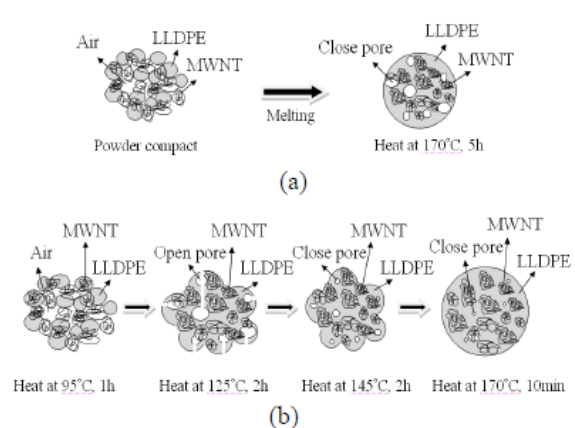


Fig. 2 Schematics of (a) single-step heating and (b) four-step heating for MWNT/LLDPE melt mixing

Under one-step heating, the porosity of the sample increased when the amount of MWNT in the MWNT/LLDPE composite was increased, as shown in Fig. 1 (a) and 2 (a). In addition, the effects of the temperature gradient caused the early surface melting of the powder compact; this was because of the high concentration of air inside the polymer melts when the powder compact was heated from room temperature to 170°C. Under four-step heating, the moisture was eliminated as

the temperature was increased from room temperature to 95°C over a period of 1 h. To melt the LLDPE—and thus to remove the air inside the open pores to form closed pores—the temperature was then raised to 125°C over a period of 2 h, as described by the Scherer and Scherer and Garino models. To ensure the complete melting of the LLDPE and the removal of the air inside the bubbles in the polymer melts, the temperature was then raised to 145°C over a period of 2 h, as shown in Fig. 1 (b) and 2 (b). To allow the polymer enough time to form a highly crystalline structure, the sample was heated to 170°C over a period of 10 min before cool naturally [2, 8]. Fig. 3 shows MWNT dispersed in the composite materials with different volume fraction percentages.

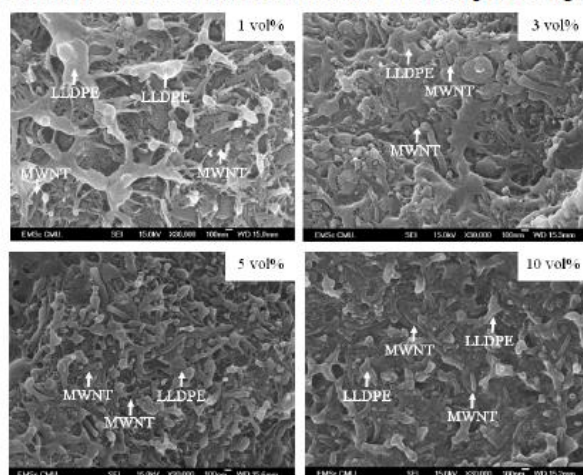


Fig. 3 SEM images of the four-step heating samples, with 1, 3, 5 and 10 vol% MWNT, respectively

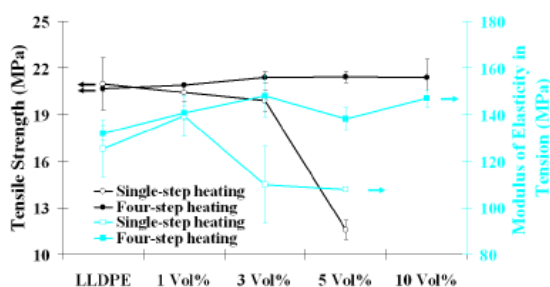


Fig. 4 Tensile Strength and Elastic Modulus of The sample prepared single and four-step heating

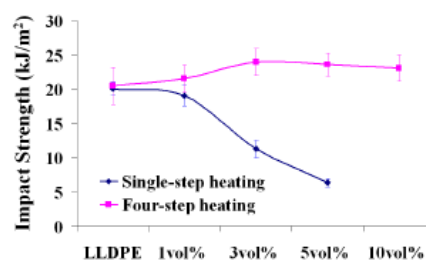


Fig. 5 Impact Strength of the sample prepared single and four-step heating

The tensile strength (Fig. 4) decreased with increased volume fraction of MWNT in the 1, 3 and 5 vol% (20.42 MPa, 19.90 MPa, and 11.58 MPa, respectively) samples prepared using single-step heating. The 10 vol% MWNT single-step heating sample could not be analyzed; because of the high porosity, it could not be pulled out of the mold. The elastic modulus values (Fig. 4) for the MWNT 1, 3 and 5 vol% samples were 139.46 MPa, 109.90 MPa, and 107.94 MPa respectively. For the samples prepared using four-step heating, the tensile strength and elastic modulus values tended to increase with increasing volume fraction of MWNT. The tensile strength values were 20.91 MPa, 21.40 MPa, 21.41 MPa, and 21.39 MPa for the 1, 3, 5 and 10 vol% MWNT samples, respectively. These values were similar to those found by Lee et al. [7]. They studied the mechanical properties of LLDPE/CNF composites with three different concentrations of CNF. The tensile strength values were approximately 20 MPa. Kuan et al. [8] investigated the tensile strength

of LLDPE/MWNT composites prepared using a water crosslinking reaction, and varied the MWNT concentration from 0 to 4 phr; the tensile strength values ranged from 19.0 to 21.7 MPa. The elastic modulus values for the sample using MWNT concentrations of 1, 3, 5 and 10 vol% were 140.68 MPa, 147.87 MPa, 138.03 MPa, and 146.81 MPa, respectively. These results occurred because the defect porosity in the single-step heating samples (Fig. 1) produced decreases in the tensile strength and elastic modulus when the MWNT volume fraction was increased in the composite materials. When four-step heating was used to melt the composite materials, this effect disappeared.

The results from the impact strength tests on the samples prepared using single- and four-step heating are shown in Fig. 5. The four-step heating samples showed increasing impact strength values with increases in the volume fraction of MWNT. The 3vol% MWNT composite showed the maximum impact strength value (23.947 kJ/m²). The four-step heating samples of 3vol% MWNT composite have optimum mechanical properties (can improve tensile strength, elastic modulus and impact strength up to 3.53%, 12.04% and 19.67%, respectively relative with pure LLDPE).

Conclusions

Using four-step heating to melt LLDPE/MWNT composites can reduce the porosity in the composite materials, resulting in increased mechanical properties in LLDPE. The 3 vol% MWNT sample prepared using four-step heating showed the highest values for tensile strength, elastic modulus, and impact strength (21.40 MPa, 147.87 MPa, and 23.947 kJ/m², respectively).

Acknowledgements

The authors gratefully acknowledge the financial support provided by Rajamangala University of Technology Lanna (RMUTL) and the National Research University Project under Thailand's office of the Commission on Higher Education (CHE) is highly appreciated.

References

- [1] M.F. Yu, O. Lourie, M.J. Dyer, K. Moloni, T.F. Kelly, R.S. Ruoff, Strength and breaking mechanism of multiwalled carbon nanotubes under tensile load, *Science*. 287 (2000) 637–640.
- [2] P.P. Kundu, J. Biswas, H. Kim, S. Choe, Influence of film preparation procedures on the crystallinity, morphology and mechanical properties of LLDPE films, *Euro. Polym. J.* 39 (2003) 1585–1593.
- [3] P. Singjai, S. Changsarn, S. Thongtem, Electrical resistivity of bulk multi-walled carbon nanotubes synthesized by an infusion chemical vapor deposition method, *Mater. Sci. Eng. A.* 443 (2007) 42-46.
- [4] L. Chen, X.J. Pang, Z.L. Yu, Study on polycarbonate/multi-walled carbon nanotubes composite produced by melt processing, *Mater. Sci. Eng. A.* 457 (2007) 287–291.
- [5] M. Kontopoulou, Polymer melt formation and densification in rotational molding, PhD thesis, McMaster University, 1999.
- [6] Y. Kong, J.N. Hay, The measurement of the crystallinity of polymer by DSC, *Polymer*. 43 (2002) 3873–3878.
- [7] S. Lee, M.S. Kim, A.A. Ogale, Influence of carbon nanofiber structure on properties of linear low density polyethylene composites, *Polym. Eng. Sci.* 50 (2010) 93-99.
- [8] C.F. Kuan, H.C. Kuan, C.C.M. Ma, C.H. Chen, H.L. Wu, The preparation of carbon nanotube/linear low density polyethylene composites by a water-crosslinking reaction, *Mater. Lett.* 61 (2007) 2744-2748.

Solar heat absorbing coating from multi-walled carbon nanotube composites with linear low-density polyethylene-coated copper sheet

Samor Boonphan and Pisith Singjai

Abstract

This study aims to investigate the effects of multi-walled carbon nanotubes (MWNTs)/linear low density polyethylene composite-coated copper sheets on an energy conversion efficiency of a solar water heating system. Volume percentages of 1, 3 and 5 MWNTs were ball-mill mixed with linear low density polyethylene before using a hot press method to coat the composites. A bonding layer between the composites and the copper sheets was intercalated using MWNTs/polyvinyl butyral composites. The strength of the bonding layer was tested using a shear tension test. Microstructures of the composites were observed by scanning electron microscopy. The energy conversion efficiency and solar absorptance of the solar heat absorbing coatings were measured by a home-made method and ultraviolet visible spectroscopy, respectively. The results showed that the efficiency and the absorptance increased by 40% and 0.95, respectively with the increasing volume percentages of MWNTs up to 5 vol.% in linear low density polyethylene.

Keywords

Composites, carbon nanotubes, mechanical properties, heat absorber

Introduction

Due to the need for pollution-free energy, there is a keen interest in finding a solution for improving the efficiency of a solar heat collector.¹ Since the solar energy is an inexpensive source of renewable energy, many research studies on this topic focus on improving the efficiency of the collector.^{2,3} The solar heat collector is utilized to absorb solar radiation and transfer heat to a medium such as water or air. There are two types of solar heat collector: a non-concentrating collector and a concentrating collector.⁴ The non-concentrating collector does not track sunlight, while the concentrating collector tracks the sunlight and transfers the solar radiation onto absorber plates. The absorber plate plays an important role among various components of the solar collectors. To improve the heat absorbing and heat transferring coefficients, the absorber plate needs to be maximized for surface roughness, thermal conductivity and density.^{5–10} Moreover, the absorber is usually painted in black because a dark surface absorbs

the thermal radiation better than a light colored surface.^{11–14} In other words, the black surface reflects a lower amount of the thermal radiation.

Carbon nanotubes (CNTs) have been proven to be an excellent thermal conductor in many applications.¹⁵ Yields from theoretical predictions show an extremely high thermal conductivity for individual single-walled carbon nanotubes (SWNTs) and multi-walled carbon nanotubes (MWNTs) at 6000 W/mK and 3000 W/mK, respectively.¹⁵ MWNTs have obvious advantages over SWNTs in aspects of low cost and ease of large-scale

Faculty of Science, Materials Science Research Center, Department of Physics and Materials Science, Chiang Mai University, Chiang Mai, Thailand

Corresponding author:

Pisith Singjai, Faculty of Science, Department of Physics and Materials Science, Chiang Mai University, 239 Huaykeaw Road, Chiang Mai 50200, Thailand.

Email: pisith.s@cmu.ac.th

production. Although there is increasing interest in the dispersion of pristine SWNTs in common organic solvents for the preparation route of the composites, the dispersion of pristine MWNTs was also widely reported.^{16–18} In addition, MWNTs were readily available in our laboratory for the purpose of this project. Furthermore, the black color of MWNTs provides a good absorbing layer for the solar radiation, combined with their high specific surface area.^{19,20} Therefore, MWNTs were usually chosen to improve the thermal properties of matrix materials.^{21–23}

Linear low density polyethylene (LLDPE) was chosen as the matrix material in this research due to its low cost and high thermal conductivity compared to other polymers. Although high density polyethylene (HDPE) has higher thermal conductivity (0.38 W/mK) than that of LLDPE (0.32 W/mK), LLDPE has been predominantly used in film and sheet applications due to its superior toughness and flexibility.^{24–26} Enhancing the properties of LLDPE should be of interest in order to expand its applications according to Krupa and Luyt, 2001.²⁷ Therefore, LLDPE has been investigated for its mechanical and thermal properties by many research groups. For example, Krupa and Luyt²⁷ reported that the thermal and mechanical properties of LLDPE were improved by a gamma radiation cross-linking.

Polyvinyl butyral (PVB) has excellent adhesive properties. It is normally used for lamination of many materials such as glass, plastics, woods, and metals.²⁸ PVB is widely used for many applications that require flexibility, toughness, and strong binding, and adheres to many surfaces such as a bonding layer in laminated safety glass for automobiles.²⁹ Moreover, PVB is used in the manufacturing process of solar panels due to its highly reliable performance under sunlight applications. Therefore, PVB is suitable for the lamination of the solar absorbing layer, whereas heat exchanging materials such as copper, aluminum, or stainless steel were normally selected.⁴

In this study, a novel absorbing plate for the solar heat collector was developed. MWNTs/LLDPE composites and MWNTs/PVB composites were prepared by using a hot press and coated on to the copper sheet. The MWNTs/LLDPE composites were coated as an absorbing layer, whereas the MWNTs/PVB composites were coated as the bonding layer. Microstructures, strength of adhesive bonding, and reflectance of the composites were investigated by scanning electron microscopy (SEM), tensile testing machine, and ultraviolet visible spectroscopy, respectively. The energy conversion efficiency of the solar heat absorbing coatings was measured by a home-made method.

Materials and methods

Synthesis of MWNTs

MWNTs were synthesized using a chemical vapor deposition (CVD) method. The length of the MWCNTs was more than 10 μm , and the diameter was approximately 20–50 nm. The resistivity of the MWNTs was 0.5–0.8 $\Omega\text{-cm}$. In comparison of the I_D/I_G ratio of the MWNTs prepared in this work with our previous work,³⁰ and other research works,^{31–33} the results showed similar structural defects. These data showed that our MWNTs were good enough for this purpose in the aspect of the comparable I_D/I_G ratio to those of other works. It is noted that I_D/I_G from the Raman spectra is the intensity ratio of the disorder-induced vibration mode (D-band) and the in-plane carbon stretching mode (G-band). Therefore, I_D/I_G is the ratio to assess the MWNT crystallinity.^{31–33}

Preparation of MWNTs/LLDPE composites and MWNTs/PVB composites

MWNTs at 1, 3, and 5 vol.% were mixed with LLDPE powders and were then ball milled for 5 h. Films of the mixing powder were then prepared by the hot press method at a pressure of 5 bars and a temperature of 180°C for 15 min. For the adhesive bonding layer, MWNTs at 10, 20, 30 and 40 vol.% were mixed with PVB in ethanol and stirred at room temperature for 24 h. MWNTs/PVB films were then prepared by a spin coating technique at 3000 r/min onto the copper sheet which was prepared according to ASTM D2651-01. Flow charts of the overall process are shown in Figure 1.

Characterizations

Microstructures of the samples were characterized by field emission scanning electron microscopy (FE-SEM: JSM 6335F). The strength of the adhesive bonding layer of the composites coated on the copper sheet was tested by the universal tensile testing machine (Hounsfield, H10KS), according to the ASTM D3164. The root mean square surface roughness (R_{rms}) of the samples was observed by atomic force microscopy (AFM: NanoScope IIIa, Digital Instruments). The reflectance of the coatings was measured by ultraviolet visible spectroscopy (VARIAN Cary 50 Conc) within a wavelength range of 190–1100 nm. The energy conversion efficiency was measured from the home-made method, the solar radiation from the sun (in a clear-sky day from 11:00 to 13:00 o'clock in April at Chiang Mai, Thailand) and a glass box of size 12 \times 12 \times 6 cm³ as schematically

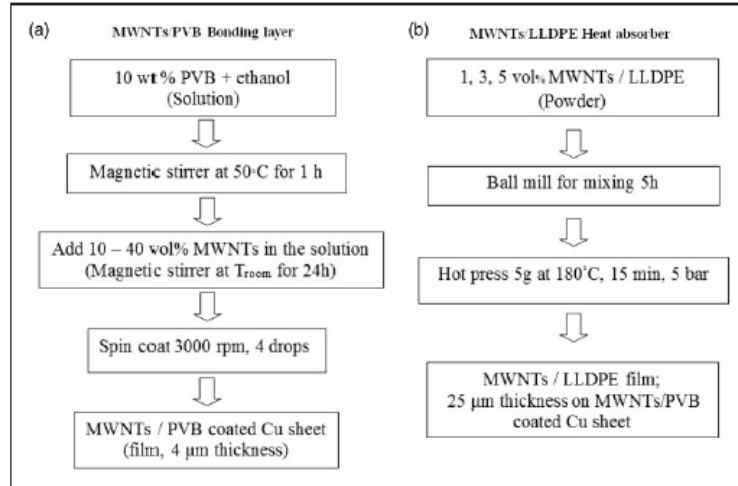


Figure 1. Flow charts showing the process of (a) MWNTs/PVB coated on a Cu sheet and (b) MWNTs/LLDPE film on MWNTs/PVB coated on a Cu sheet.

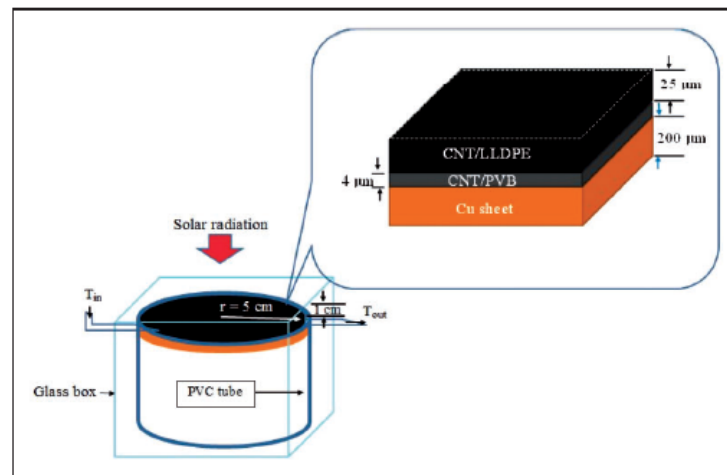


Figure 2. Schematic diagram of a home-made test system.

shown in Figure 2. The as-prepared absorber plate with a radius of 5.0 cm was placed on the top of the polyvinyl chloride (PVC) tube in the height of 5.0 cm. The solar radiation passes through the transparent glass box, before heating of the absorber plate during a water flowing over the plate at a flow rate of 3.33×10^{-5} kg/s. The temperatures of water at the inlet (T_{in}) and the outlet (T_{out}) were recorded.

Results and discussion

MWNTs/LLDPE composite

The microstructures of the MWNTs/LLDPE films prepared with various volume fractions of MWNTs were observed by SEM as shown in Figure 3(a) to (d). It can be seen in Figure 3(a) that the morphology of the pure LLDPE film was consistent with that of a normal

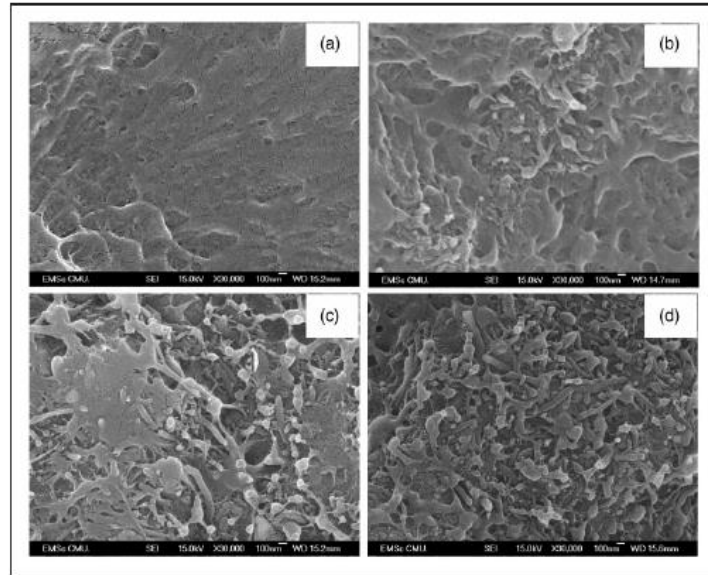


Figure 3. SEM images of MWNTs/LLDPE composites prepared with (a) 0 vol.%, (b) 1 vol.%, (c) 3 vol.%, and (d) 5 vol.% of MWNTs.

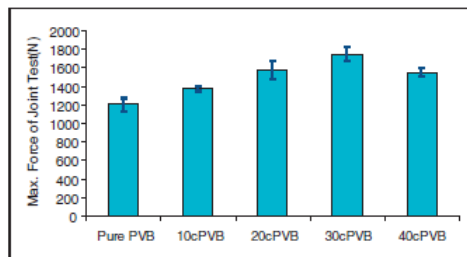


Figure 4. Joint test results of pure PVB, 10, 20, 30, and 40 vol.% MWNTs/PVB composites coated on Cu sheets.

LLDPE image.²⁷ It is noted that the MWNTs were randomly distributed into the LLDPE matrix as shown in Figure 3(b) to (d) with volume fractions of 1, 3, and 5 vol.%, respectively. MWNTs in the LLDPE matrix were evenly spread along the surface and maximized their covered fraction at 5 vol.%, as shown in Figure 3(d). However, with further increasing MWNTs by more than 5 vol.%, the porosity in the composites was clearly observed probably due to the severe agglomeration of the MWNTs.^{16,17}

MWNTs/PVB composite

The thickness of the bonding layer of $4\mu\text{m}$ was observed by SEM (data not shown). The maximum

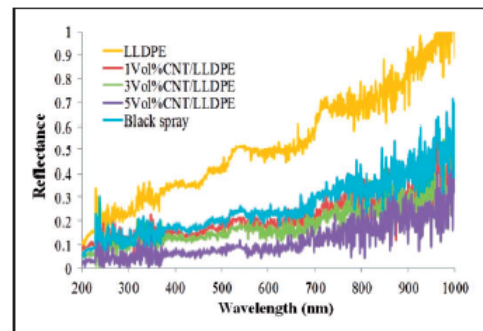


Figure 5. The reflectance spectra of MWNTs/LLDPE composites at 0, 1, 3, and 5 vol.% of MWNTs and black color spray on Cu sheets.

shearing forces for the joint test of pure PVB, and 10, 20, 30, and 40 vol.% MWNTs/PVB composite-coated copper sheets are shown in Figure 4. It is well known that the maximum force applied to the joint test increased with increasing the volume fraction of MWNTs. However, at 30 vol.%, MWNTs achieved the maximum shear strength (approximately 1800 N). It was anticipated that the effect of the agglomeration between the tubes at 40 vol.% of MWNTs started to weaken the composite strength. However, using the higher volume fraction of MWNTs provided a better

Table 1. Comparison of solar absorptance of various absorbed materials and coating methods.

| Result from | Solar absorptance (α) | Substrates | Absorbed materials | Coating methods |
|--------------------------------|--------------------------------|-----------------|------------------------------------|---|
| Cheng et al. ³⁵ | 0.949 | Copper | Carbon-titania nanocomposite films | Polymer-assisted photopolymerization-induced phase separation |
| Bera et al. ⁵ | 0.975 | Aluminum | CNT-based black coatings | Solution-processed spray |
| Feng et al. ⁶ | 0.95 | Stainless steel | TiN/TiSiN/SiN | Dc reactive magnetron sputtering |
| Roro et al. ⁹ | 0.84 | Aluminum | MWNTs/NiO nanocomposites | Sol-gel |
| Chen and Bostrom ³⁴ | 0.79–0.90 | Aluminum | CNTs | Electrophoretic |
| This work | 0.95 | Copper | MWNTs/LLDPE | Hot press |

CNT: carbon nanotube; MWNTs: multi-walled carbon nanotubes; LLDPE: linear low density polyethylene.

thermal conducting layer.²¹ Therefore, the 40 vol.% of MWNTs was applied for the bonding layer to achieve the optimum heat absorption.

Heat absorption of the MWNTs/LLDPE composite coated on Cu sheet

Figure 5 shows the spectral reflectance with four different volume fractions of MWNTs/LLDPE. The UV-Vis absorption of the MWNTs/LLDPE composites was evaluated from UV-Vis reflectance spectra using the equation: $\alpha + R + T = 1$, where α is absorptance, R is reflectance, and T is transmittance. When MWNTs/LLDPE was coated on to the copper sheet, the transmittance is about zero due to the copper sheet being opaque and therefore the absorptance is $\alpha = 1 - R$. The absorption increased with the increasing volume fraction of MWNTs reaching a maximum of 0.95 at 5 vol.% MWNTs/LLDPE.

Comparison of solar absorptance by this technique and by others is summarized in Table 1. As discussed above, the solar absorption depends on the thickness, the density, the surface roughness, and the volume fraction of the black fillers in the matrix. However, Roro et al.⁹ and Chen and Bostrom³⁴ reported that MWNT-coated aluminum substrates showed the absorptions of 0.84 and 0.79–0.90, respectively. The low absorption of these coatings was probably due to the low thickness and density of the films. In contrast with Cheng et al.,³⁵ Bera et al.⁵ and Feng et al.⁶ reported high absorptance of 0.949, 0.975, and 0.95, respectively. The high absorption of these coatings was probably due to the high thickness and high surface roughness, as well as the dispersion of the black base evenly through the matrix. For this work, the results of the coatings achieved the solar absorption of 0.95. It was anticipated that the high absorption of this coatings was due to the high surface roughness and the good distribution of MWNTs in LLDPE as shown in Figure 3(d). It is

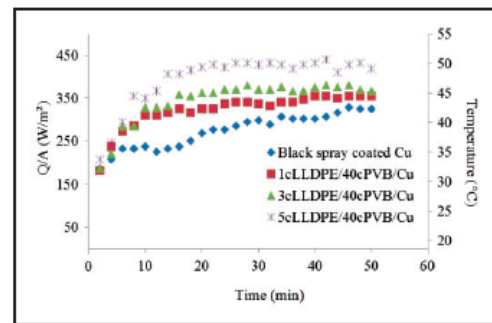


Figure 6. Energy and temperature of the water absorbed heat versus the testing time of black color spray and 1, 3, and 5 vol.% of MWNT/LLDPE composites.

known that a rough surface can improve the thermal absorption due to multiples reflections of the incoming solar radiation.^{36,37} It was found that the R_{rms} of the 1, 3, and 5 vol.% MWNT/LLDPE composites were 54.4, 66.3 and 78.3 nm, respectively. Our AFM result confirmed that the solar thermal absorption increased with increasing the rough surface.

The solar water heaters were tested, the absorbed solar radiation through the black paint and the 1, 3, and 5 vol.% MWNT/LLDPE composites with the 40 vol.% MWNT/PVB composites for the bonding layer coated on the copper sheets. The results of the sample using 5 vol.% MWNT/LLDPE composites showed a maximum temperature of 52°C. To convert the absorbed heat of water to the energy per unit area of the samples, the following equation was used

$$P = dQ/dt = (dm/dt)c_w(T_{out} - T_{in}) \quad (1)$$

where P is the power, Q is the collected solar energy, c_w is the specific heat of the water, and dm/dt is the mass

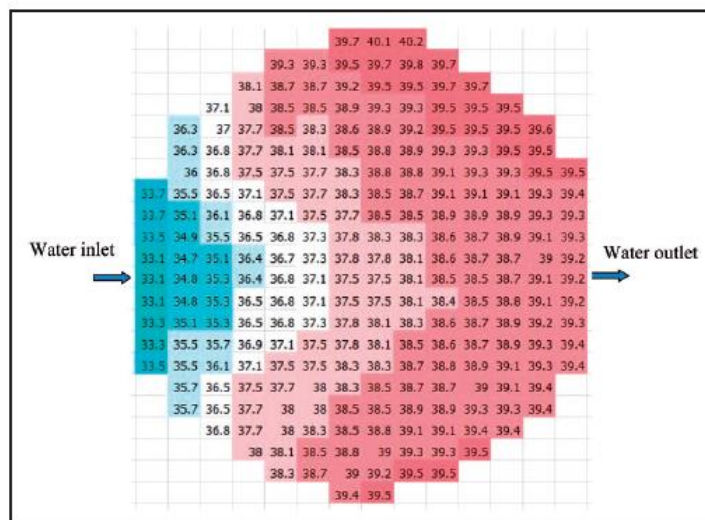


Figure 7. Temperature profile of the water as it flowed from the inlet across the surface of solar heater to the outlet.

flow rate of water. The absorbed solar power was calculated by Q over the time and the area of the solar absorber ($A = 0.007854 \text{ m}^2$). The maximum energy absorption per unit area was found in the sample using 5 vol.% MWNT/LLDPE composites of approximately 450 W/m^2 , as shown in Figure 6. In other words, the energy conversion efficiency was approximately 40%.

In addition, a method to improve the performance of the solar collector according to Eze³⁸ and Sivakumar³⁹ was a zig-zag arrangement of water pathways on the collector or a spiral loop of the absorbing tube which lead to a higher collection efficiency (42% and 53–60%, respectively). It was suggested that, to improve the performance from 40% to 60% for the solar collector, the zig-zag arrangement of the pathway should be made.

The temperatures of water were measured as it was flowing from the inlet to the outlet across the absorbing plate, as shown in Figure 7. This enabled us to develop a temperature profile of the water heater surface. It is clearly seen that the absorbed heat increased from the inlet to the outlet and also from the center to the edge of the surface due to the longer water pathways. In other words, due to the longer flowing time on the absorbing plate, the water gains more energy from the solar collector.^{38,39} Therefore, the zig-zag arrangement of MWNT/LLDPE coatings will also improve the solar conversion efficiency of the solar water heating system.

Conclusion

This paper offers the experimental results for the solar heat absorption of MWNTs/LLDPE composites coated on copper sheets. The simple hot press method was applied to prepare MWNTs/LLDPE coatings. The results showed that the MWNTs in the LLDPE were evenly spread and the surface fraction of MWNTs increased with increasing the volume ratio. Due to the nanostructures and black MWNTs as compared to other materials, the solar absorbance of the coatings was achieved at 0.95 for the sample condition at 5 vol.% MWNTs/LLDPE composites. The results also suggested that the efficiency of the novel coatings of MWNTs/LLDPE composites for use as a solar heat collector can be further improved by mixing a higher volume ratio of MWNTs as well as making the zig-zag arrangement of water pathways on the collector.

Declaration of Conflicting Interests

The author(s) declared no potential conflicts of interest with respect to the research, authorship, and/or publication of this article.

Funding

The author(s) disclosed receipt of the following financial support for the research, authorship, and/or publication of this article: The authors gratefully acknowledge the financial support provided by Rajamangala University of Technology Lanna (RMUTL) and the National Research University

Project under Thailand's office of the Commission on Higher Education (CHE).

References

- Alturaif HA, Alothman ZA, Shapter JG, et al. Use of carbon nanotubes (CNTs) with polymers in solar cells. *Molecules* 2014; 19: 17329–17344.
- Xinkang D, Cong W, Tianmin W, et al. Microstructure and spectral selectivity of Mo-Al₂O₃ solar selective absorbing coatings after annealing. 2008. *Thin Solid Film* 2008; 516: 3971–3977.
- Zhang QC and Mills DR. New cermet film structures with much improved selectivity for solar thermal applications. *Appl Phys Lett* 1992; 60: 545–547.
- Kalogirou SA. Solar thermal collectors and applications. *Prog Energy Combust Sci* 2004; 30: 231–295.
- Bera RK, Mhaisalkar SG, Mandler, et al. Formation and performance of highly absorbing solar thermal coating based on carbon nanotubes and boehmite. *Energy Convers Manage* 2016; 120: 287–293.
- Feng J, Zhang S, Liu X, et al. Solar selective absorbing coatings TiN/TiSiN/SiN prepared on stainless steel substrates. *Vacuum* 2015; 121: 135–141.
- Kim TK, Sadlers BV, Caldwell E, et al. Copper-alloyed spinel black oxides and tandem-structured solar absorbing layers for high-temperature concentrating solar power systems. *Sol Energy* 2016; 132: 257–266.
- Rincon ME, Molina JD, Sanchez M, et al. Optical characterization of tandem absorber/reflector systems based on titanium oxide-carbon coatings. *Sol Energy Mater Solar Cells* 2007; 91: 1421–1425.
- Roro KT, Tile N, Mwakikunga B, et al. Solar absorption and thermal emission properties of multiwall carbon nanotube/nickel nanocomposite thin films synthesized by sol-gel process. *Mater Sci Eng Part B* 2012; 177: 581–587.
- Yang R, Liu J, Lin L, et al. Optical properties and thermal stability of colored solar selective absorbing coatings with double-layer antireflection coatings. *Solar Energy* 2016; 125: 453–459.
- Shi H, Ok JK, Baac W, et al. Low density carbon nanotube forest as an index-matched and near perfect absorption coating. *Appl Phys Lett* 2011; 99: 211103.
- Saleh T, Moghaddam MV, Ali MSM, et al. Transforming carbon nanotube forest from darkest absorber to reflective mirror. *Phys Lett* 2012; 101: 061913.
- Xi JQ, Schubert MF, Kim JK, et al. Optical thin-film materials with low refractive index for broadband elimination of Fresnel reflection. *Nat Photo* 2007; 1: 176–179.
- Persky MJ. Review of black surfaces for space-borne infrared systems. *Rev Sci Instrum* 1999; 70: 2193–2217.
- Han Z and Fina A. Thermal conductivity of carbon nanotubes and their polymer nanocomposites: a review. *Polym Sci* 2011; 36: 914–944.
- Bokobza L. Multiwall carbon nanotube-filled natural rubber: electrical and mechanical properties. *Exp Polym Lett* 2012; 6: 213–223.
- Sun G, Liu Z and Chen G. Dispersion of pristine multi-walled carbon nanotubes in common organic solvents. *World Sci* 2010; 5: 103–109.
- Chun KY, Choi SK, Kang HJ, et al. Highly dispersed multi-walled carbon nanotubes in ethanol using potassium doping. *Carbon* 2006; 44: 1491–1495.
- Carabineiro SAC, Pereira M FR, Pereira JN, et al. Effect of the carbon nanotube surface characteristics on the conductivity and dielectric constant of carbon nanotube/poly(vinylidene fluoride) composites. *Nano Res Lett* 2011; 6: 302.
- Peigney A, Laurent C, Flahaut E, et al. Specific surface area of carbon nanotubes and bundles of carbon nanotubes. *Carbon* 2001; 39: 507–514.
- Kapadia RS, Louie BM and Bandaru PR. The influence of carbon nanotube aspect ratio on thermal conductivity enhancement in nanotube-polymer composites. *J Heat Transf* 2014; 136: 3031–3036.
- Gallego MM, Verdejo R, Khayet M, et al. Thermal conductivity of carbon nanotubes and graphene in epoxy nanofluids and nanocomposites. *Nano Res Lett* 2011; 6: 610.
- Yamanaka S, Gonda R, Kawasaki A, et al. Fabrication and thermal properties of carbon nanotube/Nickel composite by spark plasma sintering method. *Mater Transact* 2007; 48: 2506–2512.
- Dorigato A, Pegoretti A, Fambri L, et al. Linear low density polyethylene/cycloolefin copolymer blends. *Exp Polym Lett* 2011; 5: 23–37.
- Zhang H, Zhang Y, Guo W, et al. Thermal properties and morphology of recycled poly(ethylene terephthalate)/maleic anhydride grafted linear low density polyethylene blends. *J Appl Polym Sci* 2008; 109: 3546–3553.
- Khanam PN, Almaadeed MA, Ouederni M, et al. Melt processing and properties of linear low density polyethylene-graphene nanoplatelet composites. *Vacuum* 2016; 130: 63–71.
- Krupa I and Luyt AS. Thermal and mechanical properties of LLDPE cross-linked with gamma radiation. *Polym Degrad Stabil* 2001; 71: 361 – 366.
- Nakane K, Ogihara T and Ogata N. Properties of poly(vinyl butyral)/TiO₂ nanocomposites formed by sol-gel process. *Compos Part B Eng* 2004; 35: 219–222.
- Dhaliwal AK and Hay JN. The characterization of polyvinyl butyral by thermal analysis. *Thermochim Acta* 2002; 391: 245–255.
- Singjai P, Changsarn S and Thongtem S. Electrical resistivity of bulk multi-walled carbon nanotubes synthesized by an infusion chemical vapor deposition method. *Mater Sci Eng A* 2007; 443: 42–46.
- Zdrojek M, Gebicki W, Jastrzebski C, et al. Studies of multiwall carbon nanotubes using Raman spectroscopy and atomic force microscopy. *Solid State Phen* 2004; 99: 1–4.
- Lehman JH, Terrones M, Mansfield E, et al. Evaluating the characteristics of multiwall carbon nanotubes. *Carbon* 2011; 49: 2581–2602.
- Bokobza L and Zhang J. Raman spectroscopic characterization of multiwall carbon nanotubes and of composites. *Exp Polym Lett* 2012; 6: 601–608.

34. Chen Z and Bostrom T. Electrophoretically deposited carbon nanotube spectrally selective solar absorbers. *Sol Energy Mater Sol Cel* 2016; 144: 678–683.
35. Cheng B, Wang KK, Wang KP, et al. Preparation and characterization of porous carbon- titania nanocomposite films as solar selective absorbers. *J Alloy Compd* 2015; 635: 129–135.
36. Bergstrom D, Powell J and Kaplan AFH. The absorbance of steels to Nd:YLF and Nd:YAG laser light at room temperature. *Appl Surf Sci* 2007; 253: 5017–5028.
37. Ang LK, Lau YY, Gilgenbach RM, et al. Analysis of laser absorption on a rough metal surface. *Appl Phys Lett* 1997; 70: 696–698.
38. Eze JI and Ojike O. Analysis of thermal efficiency of a passive solar water heater. *Int J Phys Sci* 2012; 7: 2891–2896.
39. Sivakumar P, Christraj W, Sridharan M, et al. Performance improvement study of solar water heating system. *J Eng Appl Sci* 2012; 7: 45–49.



ลิขสิทธิ์มหาวิทยาลัยเชียงใหม่
Copyright© by Chiang Mai University
All rights reserved

CURRICULUM VITAE

Name Mr. Samor Boonphan

Date of Birth 11 September 1977

Place of Birth Nakhon Si Thammarat Province, Thailand

Academic Status 1995 High School Certificate, Pak Phanang School, Nakhon Si Thammarat, Thailand

1999 Bachelor of Science (Physics), Department of Physics, Faculty of Science, Prince of Songkla University

2003 Master of Science (Applied Physics), Department of Physics and Materials, Faculty of Science, Chiang Mai University

Scholarships Rajamangala University of Technology Lanna (RMUTL) and the National Research University Project under Thailand's office of the Commission on Higher Education (CHE)

